Received: 13 January 2017 | Revised: 9 February 2017 | Accepted: 23 February 2017
DOI: 10.1002/aoc.3804

FULL PAPER

WILEY Applied Organometallic Chemistry

Covalent supporting of novel dioxo-molybdenum tetradentate pyrrole-imine complex on Fe_3O_4 as high-efficiency nanocatalyst for selective epoxidation of olefins

Shadab Akbarpour[1] | Abolfazl Bezaatpour[1]* | Elham Askarizadeh[2]* | Mandana Amiri[1]

[1] Department of Chemistry, Faculty of Basic Science, University of Mohaghegh Ardabili 179, Ardabil, Iran
[2] Department of Applied Chemistry, Faculty of Pharmaceutical Chemistry, Pharmaceutical Science Branch, Islamic Azad University, Tehran, Iran

Correspondence
Abolfazl Bezaatpour, Department of Chemistry, Faculty of Basic Science, University of Mohaghegh, Ardabili 179, Ardabil, Iran.
Email: bezaatpour@uma.ac.ir
Elham Askarizadeh, Department of Applied Chemistry, Faculty of Pharmaceutical Chemistry, Pharmaceutical Science Branch, Islamic Azad University, Tehran, Iran.
Email: Elhamaskarizadeh@gmail.com

Funding Information
Research Council of Mohaghegh-e-Ardabili University

A novel Mo(VI) tetradentate Schiff base complex based on two pyrrole-imine donors was anchored covalently on Fe_3O_4 nanoparticles and characterized using physicochemical techniques. The catalytic epoxidation process was optimized in terms of the effects of solvent, reaction temperature, kind of oxidant and amount of oxidant and catalyst. Then the novel heterogeneous nanocatalyst was used for the efficient and selective catalytic epoxidation of internal alkenes (cyclohexene, cyclooctene, α-pinene, indene and *trans*-1,2-diphenylethene) and terminal alkenes (*n*-heptene, *n*-octene, *n*-dodecene and styrene) using *tert*-butyl hydroperoxide (70% in water) as oxidant in 1,2-dichloroethane as solvent. The prepared nanocatalyst is very effective for the selective epoxidation of *cis*-cyclooctene with 100% conversion, 100% selectivity and turnover frequency of 1098 h^{-1} in just 30 min. The magnetic nanocatalyst was easily recovered using an external magnetic field and was used subsequently at least six times without significant decrease in conversion.

KEYWORDS
epoxidation, molybdenum, nanocatalyst, pyrrole-imine, Schiff base

1 | INTRODUCTION

The transformation of olefins into epoxides gives valuable starting chemical materials for access to industrially important products such as drugs, intermediates, surfactants and epoxy resins.[1] Schiff base complexes of Mo(VI) have been intensively used as catalysts for their advantages such as being economic, stable, environmental friendly and commercially available.[2–6] *tert*-Butyl hydroperoxide (TBHP) is widely used in a variety of epoxidation processes with good thermal stability.[7–10] The recovery of a homogeneous catalyst from a reaction mixture is often difficult, has high costs and causes additional waste. Furthermore, insufficient chemical and thermal stability, leaching of the active metal into the solvent and recycling of the catalyst remain a scientific challenge.[11] These problems may be solved by replacement of homogeneous oxidation catalysts by environmental friendly heterogeneous catalysts.[12] Therefore, the support of metal complexes has been the subject of much research in catalytic fields.[13–16]

One of the main ideas for supporting of metal complexes is to anchor them onto large-surface-area inorganic materials such as zeolites and metal oxides.[17–23] Nowadays, magnetite nanoparticles are applied widely because of their unique properties including the high surface area, low toxicity, ability to be separated and biocompatibility.[24–30] Magnetic separation makes the recycling of catalysts from solution using external magnetic fields much easier than filtration and centrifugation.

Following our previous research on the catalytic activity of Schiff base complexes, herein we report the immobilization of a novel dioxomolybdenum N_4-type Schiff base

---

* These authors contributed equally to this work.

complex, derived from 9,9-bis(5-formylpyrrole-2-yl) fluorene, onto the surface of amino-modified magnetite nanoparticles. The novel catalyst (Fe_3O_4@APTMS/fluorene-SB-MoO_2) was characterized using infrared (IR) spectroscopy, scanning electron microscopy (SEM), transmission electron microscopy (TEM), diffuse reflectance spectroscopy (DRS), vibrating sample magnetometry (VSM), energy-dispersive X-ray spectroscopy (EDX), powder X-ray diffraction (XRD) and X-ray photoelectron spectroscopy (XPS), and examined for the epoxidation of internal alkenes (cyclohexene, cyclooctene, α-pinene, indene and *trans*-1,2-diphenylethene) and terminal alkenes (*n*-heptene, *n*-octene, *n*-dodecene and styrene) with TBHP (70% aqueous) as oxidant. The reusability of Fe_3O_4@APTMS/fluorene-SB-MoO_2 was also studied in the epoxidation of cyclooctene with TBHP (70% in water) in 1,2-dichloroethane for six reaction cycles.

2 | EXPERIMENTAL

2.1 | Chemicals and measurements

9-Flourenone, pyrrole, trifluoroacetic acid, phosphoryl chloride, *N,N′*-dimethylformamide, styrene, cyclohexene, α-pinene, cyclooctene, indene, 1-dodecene, 1-heptene, 1-octenee, *trans*-1,2-diphenylethene, ferrous chloride, ferric chloride, 3-aminopropyltrimethoxysilane (APTMS) and ammonia (25% *w*/w) were purchased from Merck. Proton nuclear magnetic resonance spectra were recorded using a Bruker NMR 400 (400 MHz) spectrophotometer in $CDCl_3$ solvent. CHNS analyses were performed using an elemental analyser (CHNSO-A PE 2400 series II system). Atomic absorption analysis was carried out with a Jena Analytik atomic absorption spectrometer. Analysis of oxidation products was conducted using GCs with an Agilent 7890 A with a capillary column and flame ionization detector. Column temperature was programmed between 180 and 200°C with a rate of 2°C min^{-1}. Nitrogen was used as carrier gas at 20 ml min^{-1}. IR spectra were obtained with a Spectomrx 1 Fourier transform IR spectrometer in KBr pellets over the range 400–4000 cm^{-1}. VSM was conducted with an MDKF-FORC/VSM) Megnatis-Daghigh-Kashan Co.). DRS data were recorded with a Scinco 4100 in the range 200–900 nm using barium sulfate as reference. Powder small-angle XRD studies were done using a Philips X'Pert with Cu Kα radiation (k = 1.54 Å). Surface morphology and distribution of nanoparticles were investigated via a SEM instrument (LEO 1430 VP).

2.2 | Preparation of Fe_3O_4@APTMS

Magnetite nanoparticles (Fe_3O_4) were synthesized using the chemical co-precipitation method from the literature.[31] APTMS (2.5 ml) dissolved in 50 ml of ethanol was added dropwise to the suspension of Fe_3O_4 (0.5 g) in ethanol (50 ml). After 12 h of stirring of the mixture at 70°C, the aminated magnetic nanoparticles were collected with an external magnetic field and washed with water three times. IR (KBr, cm^{-1}): 3406 [ν(O—H)], 1004 [ν(Si—O—Si)], 582 [ν(Fe—O)].

2.3 | Preparation of 9,9-Bis(5-formylpyrrole-2-yl)fluorene

9,9-Bis(5-formylpyrrole-2-yl)fluorene was prepared as reported in the literature.[32] First, 7.2 ml of fresh pyrrole was added to 3.9 g of 9-fluorenone with stirring at 0–3°C. After 10 min, trifluoroacetic acid (five drops) was added to reaction system as catalyst and the reaction mixture was kept at 0°C with stirring for 10 min. Then the reaction was stopped with the addition of 38 ml of 0.1 M sodium hydroxide and the temperature of mixture increased to ambient. The mixture was extracted with CH_2Cl_2 and dried with magnesium sulfate. Vacuum removal of CH_2Cl_2 and excess regent gave 85% yield of 9,9-bis(pyrrole-2-yl)fluorene. Subsequently,

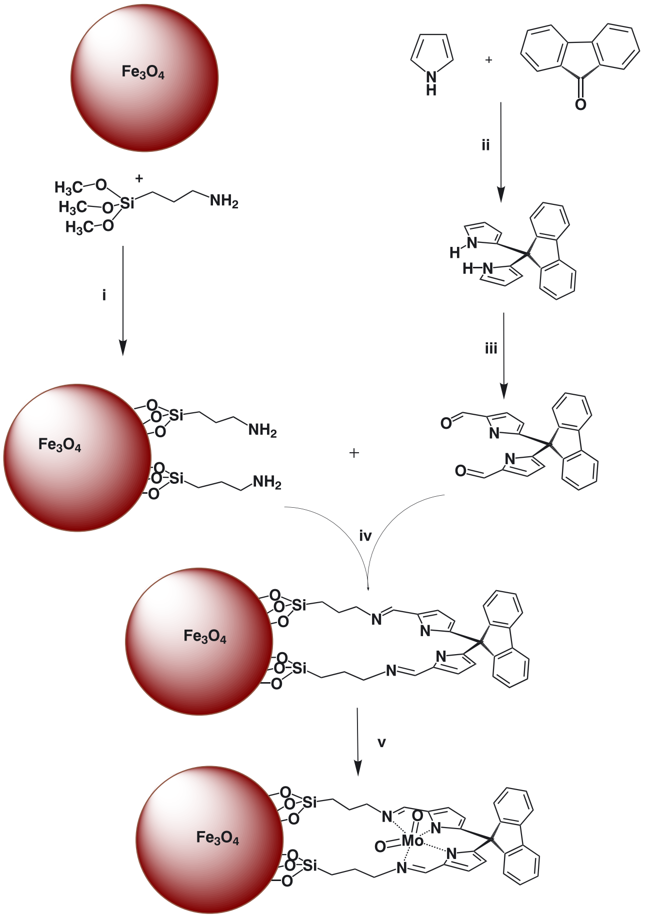

SCHEME 1 Preparation of heterogeneous nanocatalyst: (i) trifluoroacetic acid, (ii) $POCl_3$, *N,N′*-dimethylformamide, (iii) EtOH, (iv) stirring at 70 °C for 48 h, (v) $MoO_2(acac)_2$/EtOH

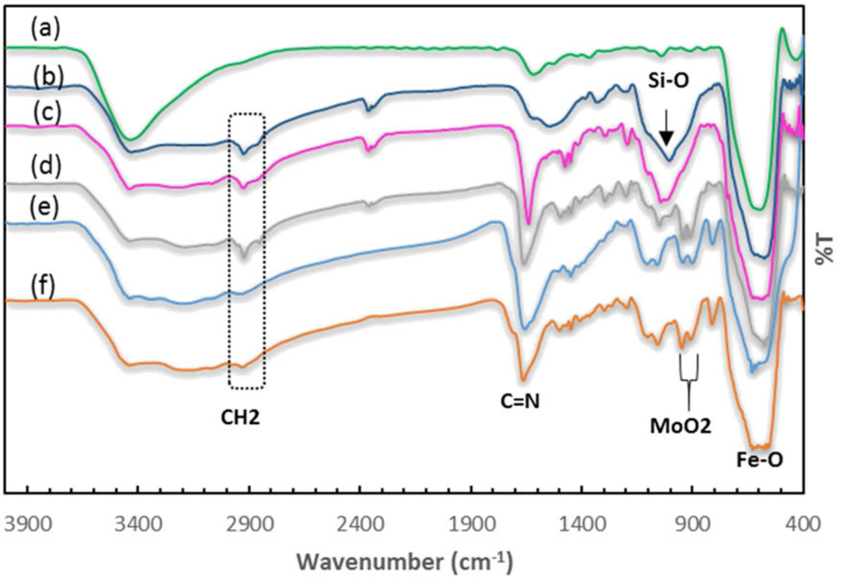

FIGURE 1 IR spectra: (a) Fe_3O_4 nanoparticles; (b) Fe_3O_4@APTMS; (c) Fe_3O_4@APTMS/fluorene-SB; (d) Fe_3O_4@APTMS/fluorene-SB-MoO_2; (e) Fe_3O_4@APTMS/fluorene-SB-MoO_2 (run 1); (f) Fe_3O_4@APTMS/fluorene-SB-MoO_2 (run 6)

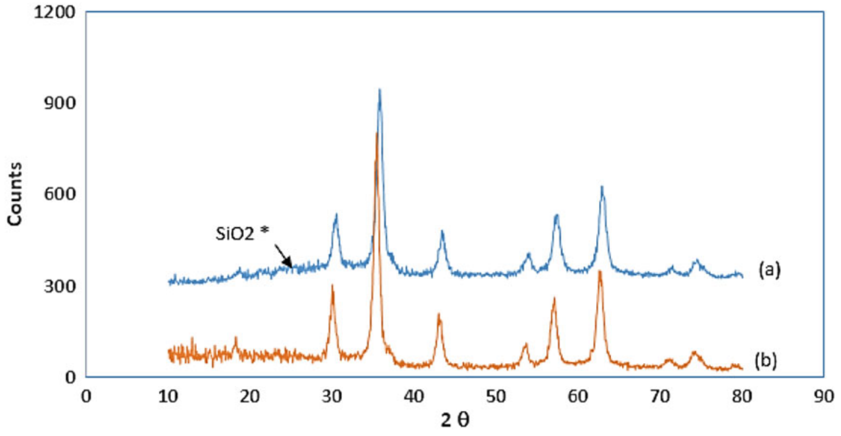

FIGURE 2 XRD patterns: (a) Fe_3O_4@APTMS/fluorene-SB-MoO_2; (b) magnetite nanoparticles

phosphoryl chloride (1.40 ml, 14.85 mmol) and 9,9-bis(pyrrole-2-yl)fluorene (1.95 g, 6.66 mmol) were mixed together in 20 ml of *N*,*N*-dimethylformamide at 0°C. After 70 min of stirring at 25°C, the reaction was quenched with addition of 38 ml of water. Then aqueous potassium hydroxide (2 M) was added until reaction mixture became strongly basic. The mixture was boiled for 50 min and a colourless precipitate obtained by filtration. The solids were washed with water three times and dried. Yield 2.06 g, 85% of 9,9-bis(5-formylpyrrole-2-yl)fluorene; m.p. 262°C. Anal. Calcd for $C_{23}H_{16}N_2O_2$ (%): C, 78.39; H, 4.58; N, 7.95. Found (%): C, 78.11; H, 4.73; N, 8.20. IR (KBr, cm^{-1}): 1649 [ν(C═O)], 3217 [ν(N─H)]. ^{1}H NMR (500 MHz, $CDCl_3$, δ, ppm): 11.53 (br, 2H, NH), 9.03 (s, 2H, CHO), 8.02 (m, 2H, fluorenyl), 7.78 (m, 2H, fluorenyl), 6.73 (d, 2H, pyrrole), 5.73 (d, 2H, pyrrole), 7.4–7.3 (m, 4H, fluorenyl) (supporting information, Figure S1). MS, *m*/*z*: 352.2 (M_A: 352.4 g mol^{-1}) (supporting information, Figure S2).

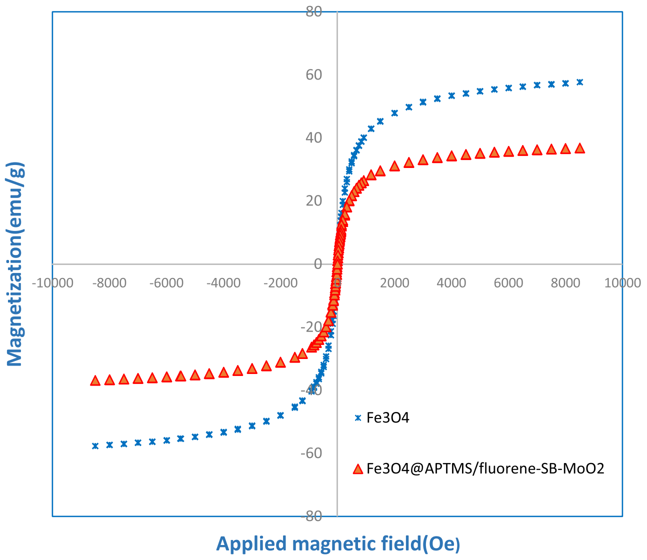

FIGURE 3 Magnetization response of Fe_3O_4@APTMS/fluorene-SB-MoO_2 at 25°C

2.4 | Preparation of Fe_3O_4@APTMS/fluorene-SB

A solution of 9,9-bis(5-formylpyrrole-2-yl)fluorene (2 g, 6 mol, in 50 ml of EtOH) was added to a suspension of Fe_3O_4@APTMS (1.0 g in 50 ml of EtOH). The mixture was stirred for 48 h at 70 °C. Then, Fe_3O_4@APTMS/fluorene-SB was collected using a magnet and washed with water and ethanol several times. IR (KBr, cm^{-1}): 586 [ν(Fe—O)], 1022 [ν(Si—O—Si)], 1640 [ν(C=N)], 2926 [C—H], 3224 [ν(N—H)], 3438 [ν(O—H)].

2.5 | Preparation of Fe_3O_4@APTMS/fluorene-SB-MoO_2

$MoO_2(acac)_2$ (1.96 g, 6 mol, in 20 ml of EtOH) was added dropwise to a suspension of 2 g of Fe_3O_4@APTMS/fluorene-SB in 40 ml of EtOH and the mixture was refluxed for 24 h. Then, the solid was separated using an external magnet and washed several times with water and ethanol. IR (KBr, cm^{-1}): 580 [ν(Fe—O)], 912, 946 [ν(*cis*, O=Mo=O)], 1052 [ν(Si—O—Si)], 1662 [ν(C=N)], 2926 [C—H], 3438 [ν(O—H)].

2.6 | Catalytic epoxidation of olefins

The catalytic activity of the heterogeneous Fe_3O_4@APTMS/fluorene-SB-MoO_2 catalyst was investigated in the epoxidation of various olefins. For this, 0.05 g of Fe_3O_4@APTMS/fluorene-SB-MoO_2 was sonicated in 5 ml of dichloroethane as solvent for 30 min. Then the substrate (0.5 mmol) and TBHP (1.0 mmol) were added in a ratio of 1:2 to the catalyst reaction. The catalytic reaction was refluxed for 30 min and the catalyst was removed using a magnet and the residue was subjected to GC analysis.

3 | RESULTS AND DISCUSSION

3.1 | Synthesis and characterization

The novel Fe_3O_4@APTMS/fluorene-SB-MoO_2 catalyst was prepared following the steps shown in Scheme 1. Figure 1 shows the IR spectra of Fe_3O_4 nanoparticles, Fe_3O_4@APTMS, anchored Schiff base ligand and Fe_3O_4@APTMS/fluorene-SB-MoO_2. As shown in Figure 1(a,b), Fe—O and Si—O stretching bands appear at 578 and 1006 cm^{-1}. The band assigned to imine stretching vibration of the anchored ligand at 1638 cm^{-1} (Figure 1c) has shifted to 1660 cm^{-1} after coordination with the Mo(VI) centre (Figure 1d).[33] The appearance of two adjacent bands at 942 and 908 cm^{-1} is characteristic of the presence of asymmetric and symmetric stretches of *cis*-[O=Mo=O] group (Figure 1d).[34] The band at 2900 cm^{-1} can be assigned to aliphatic group (CH_2) of APTMS. Considering these bands of the IR spectra confirms the anchoring of Schiff base Mo(VI) complex on magnetic nanoparticles.

As expected in the XRD pattern (Figure 2) and comparing with that of standard Fe_3O_4 nanoparticles (JCPDS card no. 87–2334), diffraction peaks are observed (220, $2\theta = 30.13°$), (331, $2\theta = 35.65°$), (400, $2\theta = 43.51°$), (422, $2\theta = 54.25°$), (511, $2\theta = 57.19°$) and (440, $2\theta = 63.13°$) for Fe_3O_4 nanoparticles and Fe_3O_4@APTMS/fluorene-SB-MoO_2. The broad peak (about $2\theta = 20.85–32°$) of Fe_3O_4@APTMS/fluorene-SB-MoO_2 is attributed to the presence of amorphous SiO_2.

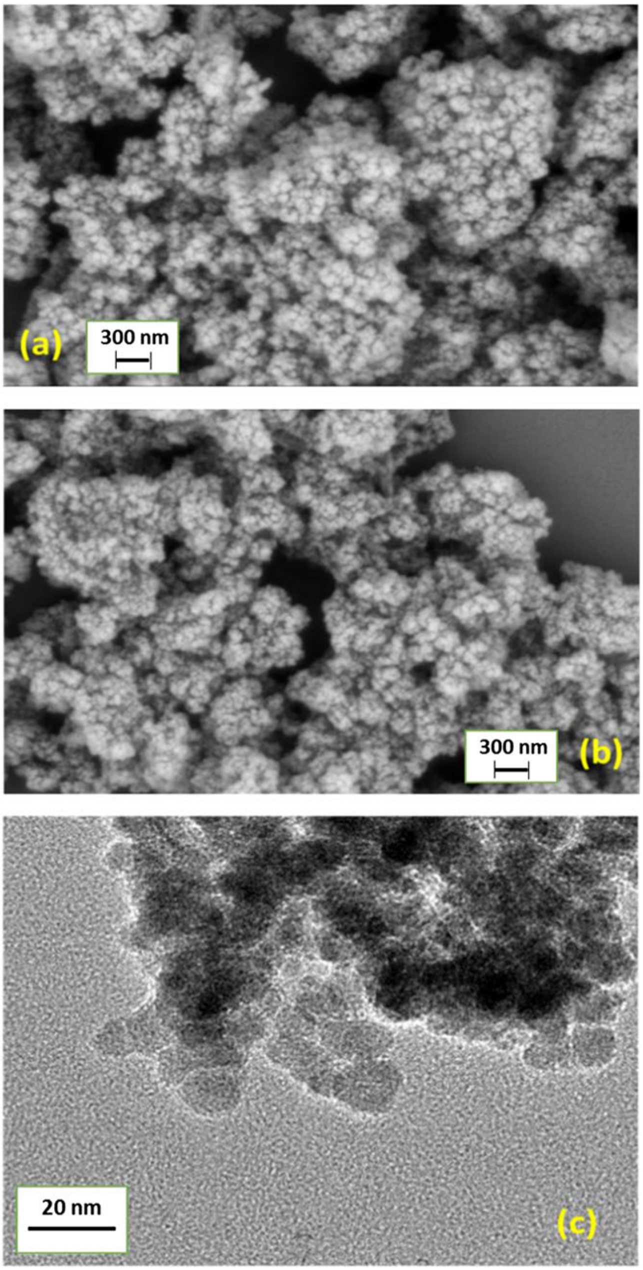

FIGURE 4 SEM images of (a) magnetite nanoparticles and (b) Fe_3O_4@APTMS/fluorene-SB-MoO_2. (c) TEM image of final catalyst

Figure 3 shows the magnetization curves of Fe_3O_4 nanoparticles and Fe_3O_4@APTMS/fluorene-SB-MoO_2. The curves show no hysteresis loops and indicate magnetic saturation at 57.67 and 36.84 emu g^{-1}, respectively. The result shows that the supporting of the catalyst on the magnetic nanoparticles decreases the magnetic saturation, but also the catalyst can be separated from the solution using a small external magnetic field.

Figure 4 shows SEM and TEM images of magnetite nanoparticles and nanocatalyst. Comparison between the SEM images of Fe_3O_4@APTMS/fluorene-SB-MoO_2 and magnetite nanoparticles shows no change in morphology. The TEM image of Fe_3O_4@APTMS/fluorene-SB-MoO_2 shows the particle size to be approximately 17–20 nm. The EDX spectrum of the catalyst indicates the presence of Mo, Si, C and the other elements on the catalyst surface (Figure 5). The XPS spectrum of Fe_3O_4@APTMS/fluorene-SB-MoO_2 catalyst is shown in Figure 6. The Fe 2p peak at 709.7 eV, O 1 s peak at 529.79 eV and Si 2p peak at 101.87 eV are as expected for Fe_3O_4/SiO_2 material. The peaks at 232.23 and 235.38 eV are assigned to Mo 3d5 and 3d3, respectively. In addition to the Mo^{6+} peaks, the peaks for N 1 s at 400.07 eV and C 1 s at 284.36 eV confirm the supporting of Mo Schiff base complex onto Fe_3O_4/SiO_2 surface. Also, XPS results of the catalyst show 3.66% loading of Mo on the surface of nanoparticles. This result is in good agreement with the atomic absorption spectrometry result (3.5% Mo).

3.2 | Epoxidation of olefins catalysed by Fe_3O_4@APTMS/fluorene-SB-MoO_2

The Fe_3O_4@APTMS/fluorene-SB-MoO_2 catalyst was used for epoxidation of internal alkenes and terminal alkenes using TBHP. Initially, various parameters such as the kind of oxidant and solvent, amount of catalyst, temperature, reaction time and molar ratio of oxidant/substrate were optimized.

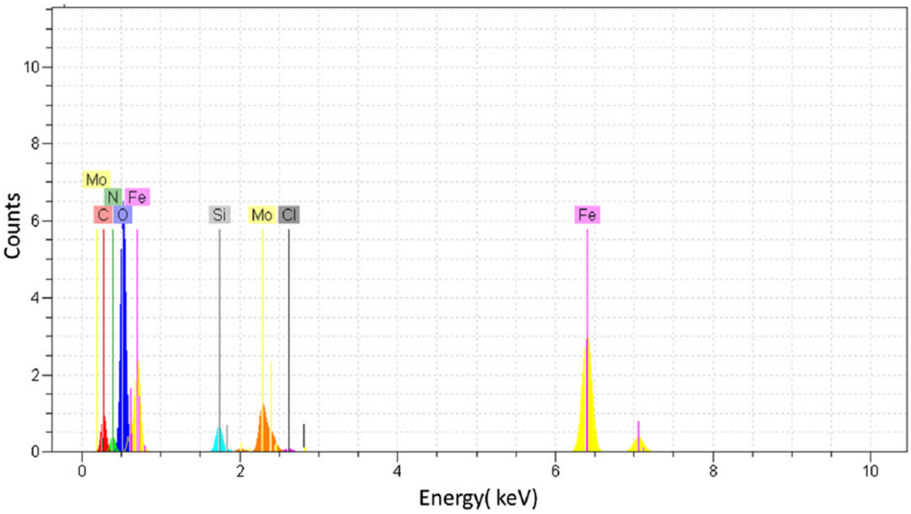

FIGURE 5 EDX spectrum of Fe_3O_4@APTMS/fluorene-SB-MoO_2

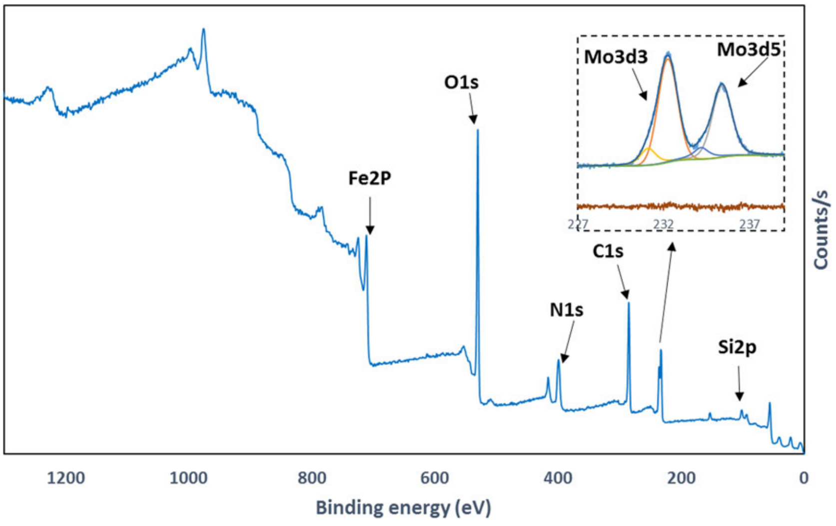

FIGURE 6 XPS spectrum of Fe_3O_4@APTMS/fluorene-SB-MoO_2

After running the catalytic process for epoxidation of cyclooctene with TBHP and various solvents, it is found that 1,2-dichloroethane is a suitable solvent among toluene, chloroform, dichloromethane, methanol and acetonitrile, with highest conversion (100%) during 30 min. By considering the mechanism shown in Scheme 2, it seems that the competition between methanol, acetonitrile as a coordinator solvent and $(CH_3)_3COO^-$ coordinated to Mo(VI) causes a marked decrease in the catalyst activity.[35] Apparently, the lower reflux reaction temperature is the reason for the lowest epoxidation conversion in CH_2Cl_2 (37%). For optimization of reaction temperature, epoxidation of cyclooctene was carried out in 1,2-dichloroethane using TBHP at four temperatures (25, 40, 60, 80°C). As evident from Table 1, the best results are obtained at 80 ± 2°C. For selecting a suitable oxidant, sodium periodate, hydrogen peroxide-urea, hydrogen peroxide and TBHP (70% in water) were tested in cyclooctene epoxidation in 1, 2-dichloroethane. As evident from Table 1, we obtained the best results in the presence of TBHP (70% in water). So TBHP has some significant advantages: (1) high selectivity; (2) unreactive towards substrate without catalyst; (3) high thermal stability. The epoxidation of cyclooctene was performed at various [TBHP]/[cyclooctene] ratios. For this, ratios of 0.5, 1, 1.5 and 2 were used in separate catalytic reactions. Figure 7 shows that the catalytic activity increased with increasing [TBHP]/[cyclooctene] ratio and the maximum conversion was observed at a ratio of in 2.0. The amount of catalyst was optimized for epoxidation of cyclooctene by using 0, 0.005, 0.010, 0.020, 0.030, 0.040 and 0.050 g of Fe_3O_4@APTMS/fluorene-SB-MoO_2. As illustrated in Figure 8, the conversion of catalyst increases with increasing amount of catalyst. Finally, 1,2-dichloroethane (5 ml) as solvent, olefin (10 mmol) as substrate, TBHP (20 mmol) as oxidant and 0.05 g of catalyst (1.82×10^{-2} mmol, determined by atomic absorption spectroscopy) at 80 ± 2 °C with stirring for 30 min were selected. By monitoring the catalyst reactor, the final solution exhibited no colour and no Mo leaching (determined by atomic absorption spectroscopy) in the solution after the catalytic procedure.

TABLE 1 Investigation of solvent, oxidant and temperature in epoxidation of cyclooctene catalysed by Fe_3O_4@APTMS/fluorene-SB-MoO_2[a]

Entry	Solvent	Oxidant	Temp. (°C)	Conversion (%)
1	$C_2H_4Cl_2$	TBHP	25	22
2	$C_2H_4Cl_2$	TBHP	40	63
3	$C_2H_4Cl_2$	TBHP	60	79
4	$C_2H_4Cl_2$	TBHP	80	100
5	$C_2H_4Cl_2$	TBHP	80	70[b]
6	$C_2H_4Cl_2$	TBHP	80	71[c]
7	$C_2H_4Cl_2$	UHP	80	39
8	$C_2H_4Cl_2$	$NaIO_4$	80	35
9	$C_2H_4Cl_2$	H_2O_2	80	45
10	CH_3CN	TBHP	80	41
11	Toluene	TBHP	80	34
12	CH_3Cl	TBHP	Reflux	80
13	CH_3OH	TBHP	Reflux	10
14	CH_2Cl_2	TBHP	Reflux	37

[a] Reaction conditions: solvent =5 ml; catalyst =1.82×10^{-2} mmol; 10 mmol alkene and 20 mmol oxidant; reaction time = 30 min.

[b] Reaction time = 15 min.

[c] Hot filtration test: after 15 min, catalyst removed from reaction mixture and conversion calculated after next 15 min.

The results of catalytic epoxidation of olefins are summarized in Table 2. Our results demonstrate 100% conversion and 100% epoxidation selectivity for cyclooctene in 30 min. So the turnover frequency of catalyst for cyclooctene

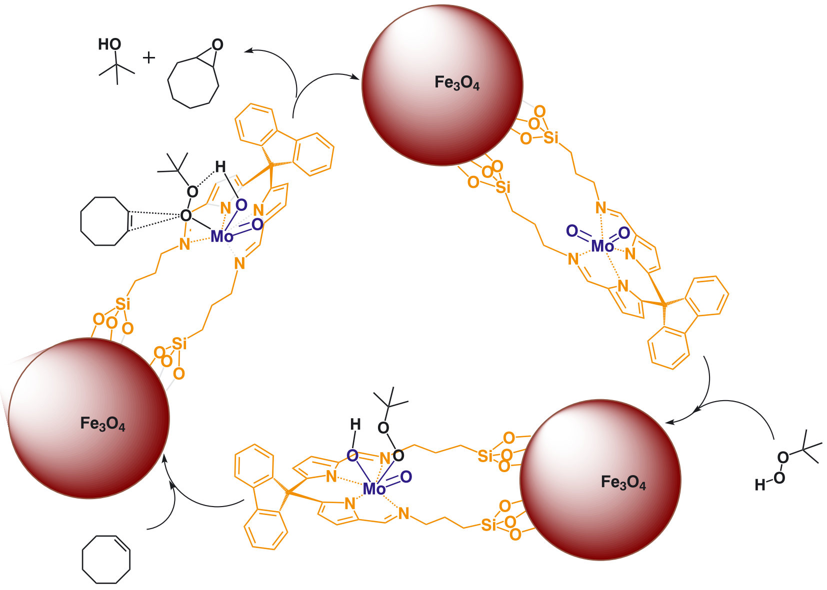

SCHEME 2 Proposed mechanism for catalytic oxidation of olefins

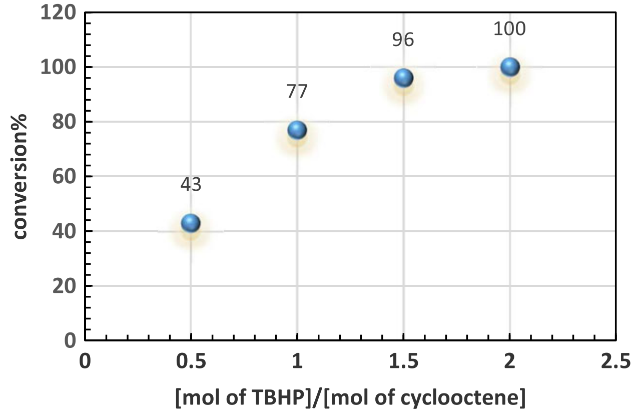

FIGURE 7 Effect of molar ratio of TBHP and cyclooctene on conversion in 1,2-dichloroethane as solvent at reflux temperature

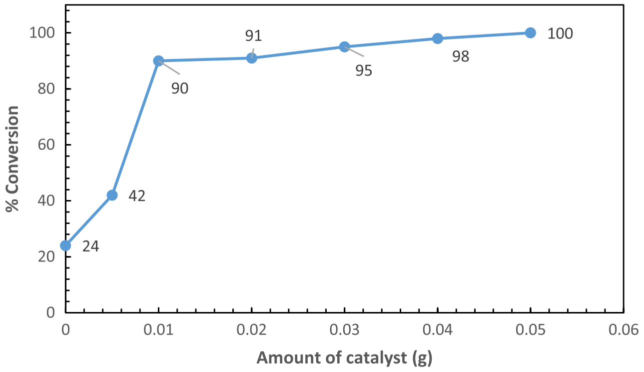

FIGURE 8 Effect of catalyst amount on cyclooctene epoxidation in 1,2-dichloroethane as solvent at reflux temperature with TBHP as oxidant

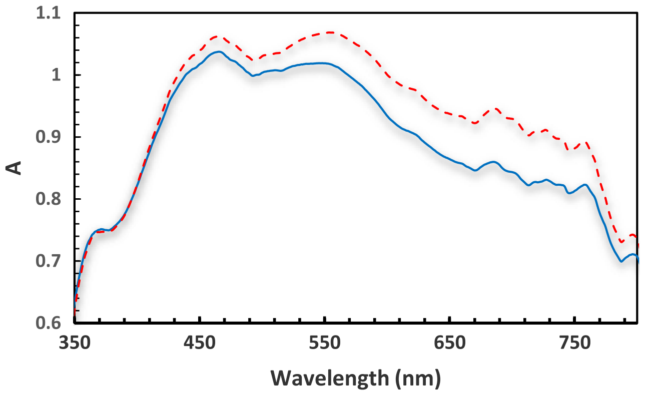

FIGURE 9 DRS spectrum of Fe_3O_4@APTMS/fluorene-SB-MoO_2 before oxidation process (solid) and Fe_3O_4@APTMS/fluorene-SB-MoO_2 after six recycles (dotted)

TABLE 3 Recycling of cyclooctene epoxidation catalyst with TBHP[a]

Run	Conversion (%)	Leaching of Mo (%)[b]
1	100	0.02
2	99	0
3	99	0.01
4	99	0
5	98	0
6	97	0

[a] Catalytic reaction conditions: 1,2-dichloroethane =5 ml; catalyst =1.82 × 10^{-2} mmol; 10 mmol alkene and 20 mmol TBHP.

[b] Monitored by atomic absorption spectroscopy.

TABLE 2 Results of catalytic epoxidation of various alkenes with TBHP catalysed by Fe_3O_4@APTMS/fluorene-SB-MoO_2[a]

Alkene	Conversion after 30 min (%)	Conversion (%) (reaction time, min)	Selectivity of epoxy (%)	TOF (h^{-1})[b]
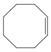	100	100 (30)	100	1098
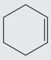	68	90 (60)	100	747
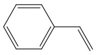	32	60 (120)	100	351
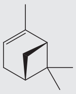	53	84 (120)	100	583
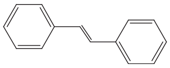	51	92 (120)	100[c] (58, 42)	561
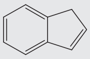	40	50 (60)	100	440
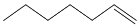	35	86 (120)	100	385
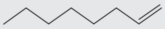	26	97 (180)	100	286
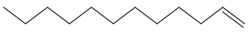	26	97 (150)	100	286

[a] Catalytic reaction conditions: 1,2-dichloroethane =5 ml; catalyst =1.82 × 10^{-2} mmol; 10 mmol alkene and 20 mmol TBHP.

[b] Calculated as [mmol of product]/[mmol of catalyst] × time.

[c] *cis*-Epoxy product: 52% and *trans*-epoxy product: 42%.

TABLE 4 Comparison of literature reports on epoxidation of cyclooctene under various conditions

Catalyst	Reaction conditions	Conversion (%)	Ref.
MoO_2–thio-Schiff base	TBHP/$CHCl_3$/24 h	36	[27]
$[MoO(O_2)_2(4\text{-MepyO})_2].H_2O$	UHP/$C_4mim(PF_6)$/18 h	90	[37]
$[MoO(O_2)_2(4\text{-MepyO})_2].H_2O$	H_2O_2/CH_3Cl/18 h	86	[38]
$[MoO(O_2)_2(H_2O)](ONnDodec_3)$	H_2O_2/CH_3Cl/2 h	25	[39]
SBA-15-MoO_2	TBHP/$C_2H_4Cl_2$/1 h	96	[40]
[MoO2(Salen)(piperazine)]$_n$	TBHP/$C_2H_4Cl_2$/12 h	95	[15]
SM-48ccg	TBHP/toluene/24 h	34	[41]
MoO_2-Salen-GO	TBHP/CH_3Cl/8 h	91.7	[5]
Dioxo-Mo(VI) acac-AmpMCM-141	TBHP/CH_3Cl/4 h	97	[42]
$[MoO_2Cl_2(\text{oep-}H_2\text{saldpen})]$	TBHP/DCE/24 h	100	[43]
Mo-IFBNPs	TBHP/CCl_4/2 h	95	[6]
Mag-Mo-Nano catalyst	TBHP/CCl_4/5 h	99	[44]
Schiff base Mo(VI) catalysts	TBHP/DCE/8 h	100	[45]
ZPS-PVPA-MoO_2	TBHP/DCE/3 h	100	[46]
MoO_2pyprMCM-41	TBHP/$CHCl_3$/4 h	75	[47]
Fe_3O_4@APTMS/fluorene-SB-MoO_2	TBHP/DCE/30 min	100	This work

epoxidation (1098 h^{-1}) is remarkable. It seems that the inclination of internal alkenes for epoxidation is more than that of terminal alkenes. The catalytic oxidation of substrate with TBHP in the blank run (without catalyst) occurs with 26% conversion. The chemical and physical stability of the catalyst allows its recycling and reuse several times (six times). The catalyst was separated easily with a magnet and used several times for the epoxidation process. As shown in Figure 1(d–f), there are no changes in the IR spectra of the catalyst before oxidation, after the second run and after the sixth run, respectively. So comparison between DRS spectra of the catalyst before and after the epoxidation process shows no change (Figure 9). The use of catalyst for several times without significant decrease in conversion and without significant leaching is evident (Table 3). Hot filtration test was performed for further investigation of catalyst leaching. For this purpose, after 15 min, the catalyst was removed from the reaction mixture and the conversion was calculated after another 15 min. As illustrated in Table 1 (entry 6), the conversion shows no significant increase. Considering the conversion results, solvent optimization and compared with previous works,[36] it seems that the proposed mechanism occurs via a seven-coordinate intermediate (Scheme 2). In respect to the mechanism in Scheme 2, it may the competition between methanol, acetonitrile as a coordinator solvent and $(CH_3)_3COO^-$ coordinated to Mo(VI) in step (II) that causes a marked decrease in the catalyst activity.[35]

Table 4 compares the present catalyst with those previously reported in the literature. In this work, we introduced a suitable magnetically separable catalytic system for epoxidation of olefins. The novel presented catalyst showed higher epoxidation catalytic activity for cyclooctene (100% conversion) than the others (36%,[27] 90%,[37] 86%[38] and 75%[39]) Finally, a comparison of catalytic reaction time and conversion of previous reports (1 h,[40] 12 h,[15] 1 day,[27,41,43] 4 h,[42] 5 h[44] and 8 h[5,45]) with that for Fe_3O_4@APTMS/fluorene-SB-MoO_2 (30 min) shows that the present catalyst is efficient and time-saving.

4 | CONCLUSIONS

We have reported the successful covalent anchoring of a novel Mo(VI) tetradentate Schiff base complex based on two pyrrole-imine donors on Fe_3O_4 nanoparticles following our pervious researches on catalytic activity. The novel paramagnetic recoverable catalyst has been studied as a nanocatalyst for selective oxidation of alkenes. The catalyst was recovered successfully using a magnet and reused as a catalyst six times without decrease in conversion and selectivity. The Fe_3O_4@APTMS/fluorene-SB-MoO_2 catalyst showed higher epoxidation catalytic activity[27,37–39] and markedly shorter catalytic reaction time than other reported catalysts.[15,27,40–45,47] The Fe_3O_4@APTMS/fluorene-SB-MoO_2 catalyst shows a highest conversion in 0.5 h.

ACKNOWLEDGEMENT

We acknowledge the Research Council of Mohaghegh-e-Ardabili University for financial support of the project.

REFERENCES

[1] Q.-H. Xia, H.-Q. Ge, C.-P. Ye, Z.-M. Liu, K.-X. Su, *Chem. Rev.* **2005**, *105*, 1603.

[2] A. Bezaatpour, S. Khatami, M. Amiri, *RSC Adv.* **2016**, *6*, 27452.

[3] G. Fioroni, F. Fringuelli, F. Pizzo, L. Vaccaro, *Green Chem.* **2003**, *5*, 425.

[4] J. Zhang, P. Jiang, Y. Shen, W. Zhang, G. Bian, *J. Porous Mater.* **2016**, *23*, 431.

[5] Z. Li, S. Wu, D. Zheng, J. Liu, H. Liu, H. Lu, Q. Huo, J. Guan, Q. Kan, *Appl. Organomet. Chem.* **2014**, *28*, 317.

[6] M. Mirzaee, B. Bahramian, A. Amoli, *Appl. Organomet. Chem.* **2015**, *29*, 593.

[7] A. Bezaatpour, *React. Kinetics Mech. Catal.* **2014**, *112*, 453.

[8] D. M. Boghaei, A. Bezaatpour, M. Behzad, *J. Mol. Catal. A* **2006**, *245*, 12.

[9] J. Rahchamani, M. Behzad, A. Bezaatpour, V. Jahed, G. Dutkiewicz, M. Kubicki, M. Salehi, *Polyhedron* **2011**, *30*, 2611.

[10] L. Canali, D. C. Sherrington, *Chem. Soc. Rev.* **1999**, *28*, 85.

[11] R. Dileep, B. Rudresha, *RSC Adv.* **2015**, *5*, 65870.

[12] A. Mavrogiorgou, M. Baikousi, V. Costas, E. Mouzourakis, Y. Deligiannakis, M. Karakassides, M. Louloudi, *J. Mol. Catal. A* **2016**, *413*, 40.

[13] A. Bezaatpour, M. Amiri, V. Jahed, *J. Coord. Chem.* **2011**, *64*, 1837.

[14] L. Hamidipour, F. Farzaneh, *C. R. Chim.* **2014**, *17*, 927.

[15] M. Bagherzadeh, M. Zare, *J. Coord. Chem.* **2013**, *66*, 2885.

[16] C. Baleizão, B. Gigante, D. Das, M. Álvaro, H. Garcia, A. Corma, *J. Catal.* **2004**, *223*, 106.

[17] A. Bezaatpour, M. Behzad, V. Jahed, M. Amiri, Y. Mansoori, Z. Rajabalizadeh, S. Sarvi, *React. Kinetics Mech. Catal.* **2012**, *107*, 367.

[18] M. Fadhli, I. Khedher, J. M. Fraile, *J. Mol. Catal. A* **2016**, *420*, 282.

[19] S. P. Shylesh, M. Jia, A. Seifert, S. Adappa, S. Ernst, W. R. Thiel, *New J. Chem.* **2009**, *33*, 717.

[20] A. M. Garcia, V. Moreno, S. X. Delgado, A. E. Ramírez, L. A. Vargas, M. Á. Vicente, A. Gil, L. A. Galeano, *J. Mol. Catal. A* **2016**, *416*, 10.

[21] J. Zhang, P. Jiang, Y. Shen, W. Zhang, X. Li, *Micropor. Mesopor. Mater.* **2015**, *206*, 161.

[22] P. Piaggio, P. McMorn, C. Langham, D. Bethell, P. C. Bulman-Page, F. E. Hancock, G. J. Hutchings, *New J. Chem.* **1998**, *22*, 1167.

[23] T. Chattopadhyay, A. Chakraborty, S. Dasgupta, A. Dutta, M. I. Menéndez, E. Zangrando, *Appl. Organomet. Chem.* **2016**, https://doi.org/10.1002/aoc.3663.

[24] P. B. Bhat, B. R. Bhat, *New J. Chem.* **2015**, *39*, 273.

[25] A. Farokhi, H. Hosseini-Monfared, *New J. Chem.* **2016**, *40*, 5032.

[26] J. Sun, G. Yu, L. Liu, Z. Li, Q. Kan, Q. Huo, J. Guan, *Catal. Sci. Technol.* **2014**, *4*, 1246.

[27] M. Mohammadikish, M. Masteri-Farahani, S. Mahdavi, *J. Magn. Magn. Mater.* **2014**, *354*, 317.

[28] T. Li, C. Yang, X. Rao, F. Xiao, J. Wang, X. Su, *Ceram. Int.* **2015**, *41*, 2214.

[29] C. I. Fernandes, M. D. Carvalho, L. P. Ferreira, C. D. Nunes, P. D. Vaz, *J. Organomet. Chem.* **2014**, *760*, 2.

[30] X. Zhang, G. Wang, M. Yang, Y. Luan, W. Dong, R. Dang, H. Gao, J. Yu, *Catal. Sci. Technol.* **2014**, *4*, 3082.

[31] Z. Peng, K. Hidajat, M. Uddin, *J. Colloid Interface Sci.* **2004**, *271*, 277.

[32] E. Askarizadeh, A. M. Devoille, D. M. Boghaei, A. M. Slawin, J. B. Love, *Inorg. Chem.* **2009**, *48*, 7491.

[33] W. Hill, N. Atabay, C. McAuliffe, F. McCullough, S. Razzoki, *Inorg. Chim. Acta* **1979**, *35*, 35.

[34] J. Topich, *Inorg. Chem.* **1981**, *20*, 3704.

[35] M. Bagherzadeh, M. Zare, V. Amani, A. Ellern, L. K. Woo, *Polyhedron* **2013**, *53*, 223.

[36] F. E. Kühn, M. Groarke, É. Bencze, E. Herdtweck, A. Prazeres, A. M. Santos, M. J. Calhorda, C. C. Romão, I. S. Gonçalves, A. D. Lopes, *Chem. – Eur. J.* **2002**, *8*, 2370.

[37] M. Herbert, F. Montilla, R. Moyano, A. Pastor, E. Álvarez, A. Galindo, *Polyhedron* **2009**, *28*, 3929.

[38] M. Herbert, F. Montilla, A. Galindo, *J. Mol. Catal. A* **2011**, *338*, 111.

[39] G. Wahl, D. Kleinhenz, A. Schorm, J. Sundermeyer, R. Stowasser, C. Rummey, G. Bringmann, C. Fickert, W. Kiefer, *Chem. – Eur. J.* **1999**, *5*, 3237.

[40] M. Bagherzadeh, M. Zare, M. Amini, T. Salemnoush, S. Akbayrak, S. Özkar, *J. Mol. Catal. A* **2014**, *395*, 470.

[41] A. Sakthivel, J. Zhao, G. Raudaschl-Sieber, M. Hanzlik, A. S. Chiang, F. E. Kühn, *Appl. Catal. A* **2005**, *281*, 267.

[42] M. Masteri-Farahani, F. Farzaneh, M. Ghandi, *J. Mol. Catal. A* **2006**, *248*, 53.

[43] S. M. Bruno, S. S. Balula, A. A. Valente, F. A. A. Paz, M. Pillinger, C. Sousa, J. Klinowski, C. Freire, P. Ribeiro-Claro, I. S. Gonçalves, *J. Mol. Catal. A* **2007**, *270*, 185.

[44] M. Shokouhimehr, Y. Piao, J. Kim, Y. Jang, T. Hyeon, *Angew. Chem. Int. Ed.* **2007**, *46*, 7039.

[45] Y. Li, X. Fu, B. Gong, X. Zou, X. Tu, J. Chen, *J. Mol. Catal. A* **2010**, *322*, 55.

[46] Z. Hu, X. Fu, Y. Li, X. Tu, *Appl. Organomet. Chem.* **2011**, *25*, 128.

[47] M. Masteri-Farahani, F. Farzaneh, M. Ghandi, *Cat. Com.* **2007**, *8*, 6.

SUPPORTING INFORMATION

Additional Supporting Information may be found online in the supporting information tab for this article.

How to cite this article: Akbarpour S, Bezaatpour A, Askarizadeh E, Amiri M. Covalent supporting of novel dioxo-molybdenum tetradentate pyrrole-imine complex on Fe3O4 as high-efficiency nanocatalyst for selective epoxidation of olefins. *Appl Organometal Chem*. 2017;e3804. https://doi.org/10.1002/aoc.3804